doi:10.1093/jmcb/mjs001
Published online January 11, 2012

Article

Activation of the cold-sensing TRPM8 channel triggers UCP1-dependent thermogenesis and prevents obesity

Shuangtao Ma[1,†], Hao Yu[1,†], Zhigang Zhao[1,†], Zhidan Luo[1], Jing Chen[1], Yinxing Ni[1], Rongbing Jin[1], Liqun Ma[1], Peijian Wang[1], Zhenyu Zhu[1], Li Li[1], Jian Zhong[1], Daoyan Liu[1], Bernd Nilius[2], and Zhiming Zhu[1,*]

[1] Center for Hypertension and Metabolic Diseases, Department of Hypertension and Endocrinology, Daping Hospital, Third Military Medical University, Chongqing Institute of Hypertension, Chongqing 400042, China
[2] KU Leuven, Department of Molecular Cell Biology, Laboratory Ion Channel Research, Campus Gasthuisberg, Herestraat 49, bus 802, Leuven, Belgium
[†] These authors contributed equally to this work.
[*] Correspondence to: Zhiming Zhu, E-mail: zhuzm@yahoo.com

Brown adipose tissue (BAT) is an energy-expending organ that produces heat. Expansion or activation of BAT prevents obesity and diabetes. Chronic cold exposure enhances thermogenesis in BAT through uncoupling protein 1 (UCP1) activation triggered via a β-adrenergic pathway. Here, we report that the cold-sensing transient receptor potential melastatin 8 (TRPM8) is functionally present in mouse BAT. Challenging brown adipocytes with menthol, a TRPM8 agonist, up-regulates UCP1 expression and requires protein kinase A activation. Upon mimicking long-term cold exposure with chronic dietary menthol application, menthol significantly increased the core temperatures and locomotor activity in wild-type mice; these effects were absent in both TRPM8$^{-/-}$ and UCP1$^{-/-}$ mice. Dietary obesity and glucose abnormalities were also prevented by menthol treatment. Our results reveal a previously unrecognized role for TRPM8, suggesting that stimulation of this channel mediates BAT thermogenesis, which could constitute a promising way to treat obesity.

Keywords: TRPM8, uncoupling protein 1, menthol, thermogenesis, brown adipose tissue, obesity

Introduction

The prevalence of obesity has increased in worldwide. Obesity develops when energy intake exceeds energy expenditure (Speakman, 2010). Enhancement of energy expenditure has emerged as a potential and attractive strategy for treating or preventing obesity (Fruhbeck et al., 2009a). Distinct from white adipose tissue (WAT), brown adipose tissue (BAT) is responsible for energy expenditure through uncoupling protein 1 (UCP1)-induced thermogenesis (Cannon and Nedergaard, 2004; Feldmann et al., 2009; Enerback, 2010). UCP1 is found exclusively in the inner membranes of the mitochondria of brown adipocytes. When activated, UCP1 uncouples the respiratory chain, and heat is generated (Nedergaard et al., 2005; Feldmann et al., 2009). BAT was originally identified in infants and rodents, but recent studies have found functional BAT in adult humans (Fruhbeck et al., 2009a; Lidell and Enerback, 2010). This novel finding highlights the crucial roles of BAT in the regulation of energy metabolism and fat deposition (Nedergaard and Cannon, 2010; Nedergaard et al., 2011). There are two sources of BAT. It appears as discrete brown fat depots during foetal development and as diffuse populations in traditional white fat depots during post-natal development, which can be induced by adrenergic stimulation (Frontini and Cinti, 2010). Recently, the transcriptional control and development of BAT have attracted substantial interest (Seale et al., 2009). However, it remains unknown whether BAT can play a role in combating obesity. It is well known that chronic exposure to cold stimulation can activate BAT and that it can up-regulate UCP1 through activation of the β3-adrenoceptor and increasing the metabolic rate (Cannon and Nedergaard, 2004). However, β-adrenoceptor deficient mice exhibited normophagic obesity and unchanged BAT UCP1 levels at temperatures slightly below thermoneutrality (Lehr et al., 2006). This result challenges the idea that β-adrenoceptor signalling is an absolute requirement for UCP1 up-regulation in BAT. Furthermore, clinical trials with β3-adrenergic receptor agonists for the treatment of obesity in humans have been disappointing because of the lack of effects on energy metabolism (Redman et al., 2007). Thus, it is important to unravel novel pathways of expansion and/or activation of BAT beyond β-adrenergic activation.

The transient receptor potential melastatin 8 (TRPM8) channel is a cold-sensing non-selective cation channel that is expressed in

Received October 2, 2011. Revised November 18, 2011. Accepted December 7, 2011

a subset of pain- and temperature-sensing neurons (Voets et al., 2004; Nilius et al., 2007a). TRPM8 can be also activated by cooling agents, such as menthol and icilin (Peier et al., 2002; Mahieu et al., 2007). TRPM8$^{-/-}$ mice display a defective response to cooling agents and cold stimuli, which indicates that this cold-sensing channel plays a physiologically relevant role in the detection of environmental temperature in mammals (Bautista et al., 2007; Colburn et al., 2007; Dhaka et al., 2007; Nilius et al., 2007b; Voets et al., 2007). Therefore, it is intriguing to hypothesize that TRPM8 activation that mimics cold exposure may also induce weight loss. It is still unknown whether activation of TRPM8 can affect BAT function through cooling agents. Here, we show that TRPM8 activation can trigger UCP1-induced non-shivering thermogenesis and locomotor activity, which prevents the development of obesity.

Results

Activation of TRPM8 enhances UCP1 production in BAT

TRPM8 is mainly expressed in sensory nerves, dorsal root ganglia (DRG), the central nervous system, the bladder and blood vessels (Peier et al., 2002). It is unknown whether TRPM8 is expressed in non-excitable tissues, such as adipose tissue. First, using DRG as a positive control, we performed immunoblotting to show that TRPM8 is expressed in BAT and in primary cultured brown adipocytes from WT mice but that it is absent in brown adipocytes from TRPM8$^{-/-}$ mice (Figure 1A). The activation of TRPM8, a Ca^{2+}-permeable non-selective cation channel, causes an increase in the cytosolic free Ca^{2+} concentration ($[Ca^{2+}]_i$) (McKemy et al., 2002). Thus, we loaded brown adipocytes with the Ca^{2+} indicator Fura-2 AM. The ratio of fluorescence intensity at 340 nm to that at 380 nm reflected changes in the $[Ca^{2+}]_i$ and demonstrated that menthol, the TRPM8 agonist, markedly increased Ca^{2+} in WT brown adipocytes, with only a very slight increase in TRPM8$^{-/-}$ cells (Figure 1B). We then evaluated whether the activation of TRPM8 by cooling agents affects UCP1 production in BAT. Immunofluorescence staining revealed the colocalization of UCP1 and TRPM8 in brown adipocytes (Figure 1C). The brown adipocytes primarily cultured from TRPM8$^{-/-}$ mice were used as a negative control (Supplementary Figure S1). When we challenged cultured brown adipocytes with menthol, UCP1 expression increased in cultured brown adipocytes from WT mice but not in those from TRPM8$^{-/-}$ mice (Figure 1D). Increased UCP1 expression was also identified in BAT from WT mice treated with dietary menthol for 7 months but not in TRPM8$^{-/-}$ mice with the same menthol treatment (Figure 1E). These findings suggest that TRPM8 is functionally expressed in brown adipocytes. The activation of TRPM8 by menthol up-regulates UCP1 levels in brown adipocytes *in vitro* and in BAT *in vivo*.

TRPM8-mediated UCP1 production is associated with protein kinase A phosphorylation

We next determined which mechanism is responsible for TRPM8-mediated UCP1 expression. Previous studies have shown that UCP1 activity and expression could be modulated by the β3-adrenoceptor pathway, PGC-1 and kinases, including phosphatidylinositol 3-kinase (PI3K), protein kinase A (PKA),

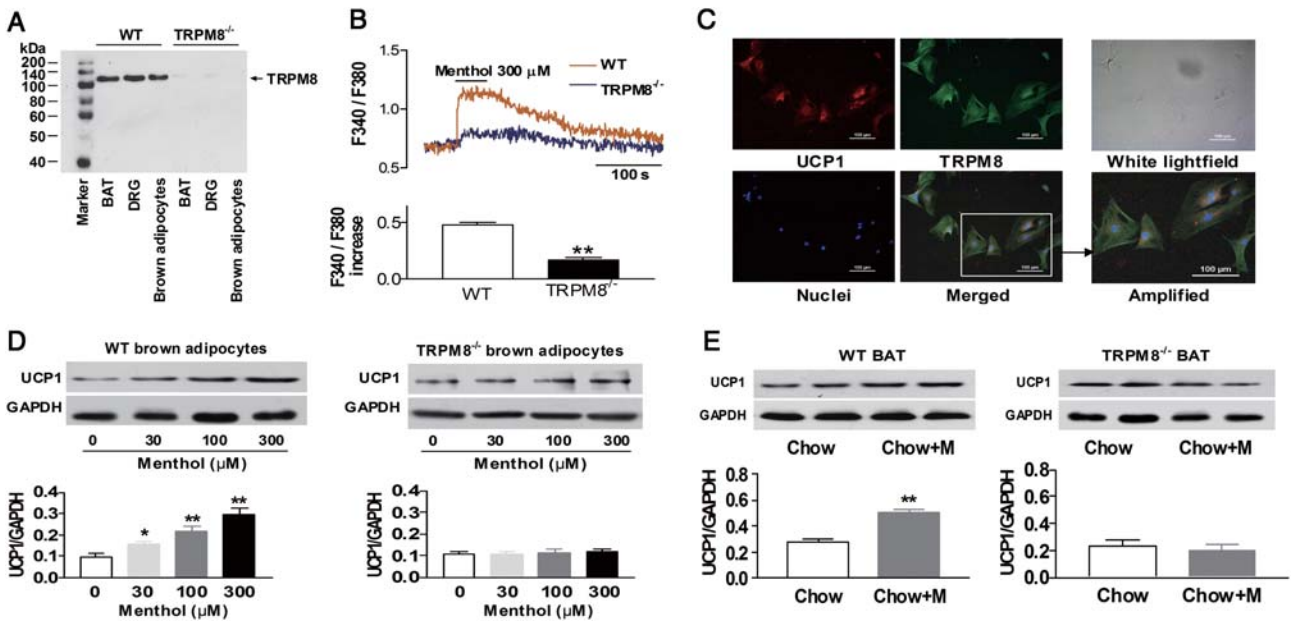

Figure 1 Effects of TRPM8 activation on the expression of UCP1 in brown adipocytes. (**A**) Immunoblotting of TRPM8 protein in DRG, BAT and primarily cultured brown adipocytes from WT and TRPM8$^{-/-}$ mice. (**B**) Effects of menthol on cytosolic Ca^{2+} concentrations in brown adipocytes primarily cultured from WT and TRPM8$^{-/-}$ mice. Representative tracings of the fluorescence ratio F340/F380 (top panel) and the summary data of the increases in ratios (bottom panel) are shown. (**C**) Immunofluorescence staining showing the colocalization of TRPM8 and UCP1 in brown adipocytes. (**D**) Dose-dependent effect of menthol on UCP1 protein expression in brown adipocytes primarily cultured from WT (left panel) and TRPM8$^{-/-}$ (right panel) mice. * $P < 0.05$, ** $P < 0.01$ vs control. (**E**) Effect of dietary menthol on UCP1 protein expression in the brown fat of WT (left panel) and TRPM8$^{-/-}$ (right panel) mice. Mice were fed standard chow diet without (Chow) or with 0.5% menthol (Chow + M) for 7 months. **$P < 0.01$ vs Chow. Data are expressed as mean ± SEM from three to five independent experiments or mice.

and AMPK (Fredriksson et al., 2001; Karamitri et al., 2009; Christian and Parker, 2010). PKA also modulates TRPM8 activity in sensory neurons from rat DRG and in HEK-293 cells (De Petrocellis et al., 2007; Bavencoffe et al., 2010). We challenged brown adipocytes with different protein kinase inhibitors and determined that LY294002, an inhibitor of PI3K, and compound C, an AMPK inhibitor, did not change menthol-induced UCP1 expression; however, the inhibition of PKA using KT5720 significantly reduced the menthol effect (Figure 2A). We further showed that administration of menthol significantly increased PKA phosphorylation in WT brown adipocytes. In contrast, the effect of menthol on PKA phosphorylation was absent in TRPM8$^{-/-}$ brown adipocytes (Figure 2B). The administration of menthol did not affect the expression of PGC-1 in BAT (Figure 2C). PPARγ, a member of the nuclear hormone receptor superfamily, plays a central role in adipocyte differentiation (Li et al., 2008). Bone morphogenetic protein 7 (BMP7), a member of the transforming growth factor-β family of proteins, has the potential to induce the differentiation of brown preadipocytes into functional brown adipocytes (Tseng et al., 2008). It has been shown that menthol treatment had no effect on PPARγ and BMP7 expression in BAT (Figure 2C), suggesting that BAT differentiation might not be affected. To identify the roles of Ca^{2+} and β-adrenoceptors in the menthol effect, we treated brown adipocytes with menthol in the presence of 1,2-*bis*(*o*-aminophenoxy)ethane-*N*,*N*,*N*′,*N*′-tetraacetic acid (BAPTA), a cytosolic Ca^{2+} chelator, or propranolol, a β-adrenoceptor antagonist. We determined that Ca^{2+} depletion significantly blocked UCP1 up-regulation and PKA phosphorylation; β-adrenoceptor inhibition produced no change in the menthol effect (Figure 2D). However, β-adrenoceptor inhibition blocked the effect of norepinephrine (Figure 2D). These results indicated that menthol could act directly on brown adipocytes through a pathway independent of β-adrenoceptors and that is distinct from traditional neurotransmitter mechanisms. Taken together, these findings suggest that the Ca^{2+}-dependent PKA phosphorylation is crucial for TRPM8-mediated UCP1 production in BAT.

Chronic activation of TRPM8 enhances UCP1-dependent thermogenesis and locomotor activity

Energy expenditure consists of the energy consumed through basal metabolism and physical activities (Sweeting, 2008). UCP1 is located in the inner mitochondrial membrane and enhances proton conductivity, subsequently resulting in the uncoupling of the electron transport system and heat production (Rousset et al., 2004). We determined whether the activation of TRPM8 could change UCP1-dependent thermogenesis and energy expenditure and showed that dietary menthol markedly increased the locomotor activities of WT mice; this effect was absent in TRPM8$^{-/-}$ mice (Figure 3A). Consistent with the increased locomotor activities, menthol treatment significantly increased the rectal temperatures in WT mice but not in TRPM8$^{-/-}$ mice (Figure 3B). Similar results were obtained in the measurements of 24-h ambulatory core body temperatures. During the day-time, core temperatures were not different; however, during the night-time, core temperatures were significantly higher in WT mice on the menthol diet compared with mice on the chow diet. However, this temperature-elevating effect of menthol was not significant in TRPM8$^{-/-}$ mice; at two time points, menthol even lowered their core temperatures (Figure 3C). We also measured the resting oxygen consumption

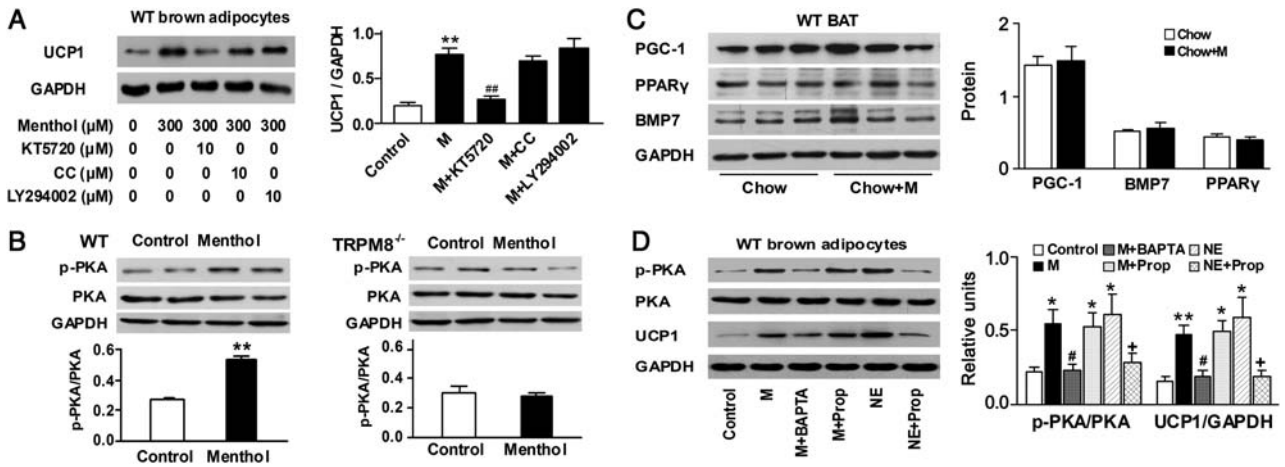

Figure 2 TRPM8-mediated UCP1 expression was associated with Ca^{2+}-dependent PKA phosphorylation. (**A**) The representative immunoblotting and summary data of UCP1 protein expression in brown adipocytes treated with menthol (300 μM) for 24 h in the presence or absence of antagonists for PKA (KT5720, 10 μM), AMPK (compound C, 10 μM), or PI3K (LY294002, 10 μM). M, menthol; CC, compound C. $^{**}P < 0.01$ vs control; $^{\#\#}P < 0.01$ vs menthol (M). (**B**) Protein levels of phosphorylated PKA (p-PKA) and total PKA (PKA) in WT (left panel) and TRPM8$^{-/-}$ (right panel) brown adipocytes treated with or without menthol (300 μM) for 24 h. $^{**}P < 0.01$ vs control. (**C**) Protein expression of PGC-1, PPARγ, and BMP7 in the brown fat of WT mice fed on chow diet without (Chow) or with 0.5% menthol (Chow + M) for 7 months. (**D**) Representative immunoblotting images (left panel) and summary data of the protein levels (right panel) of p-PKA, PKA, and UCP1 in WT brown adipocytes. Cells were treated with menthol (M, 300 μM) for 24 h in the presence or absence of the cytosolic Ca^{2+} chelator BAPTA-AM (BAPTA, 10 μM) or the β-blocker propranolol (Prop, 10 μM). Cells were also treated with norepinephrine (NE, 10 μM) with or without the presence of propranolol (10 μM). $^{*}P < 0.05$, $^{**}P < 0.01$ vs control; $^{\#}P < 0.05$ vs menthol (M); $^{+}P < 0.05$ vs NE. Data are expressed as mean ± SEM from three to five independent experiments or mice.

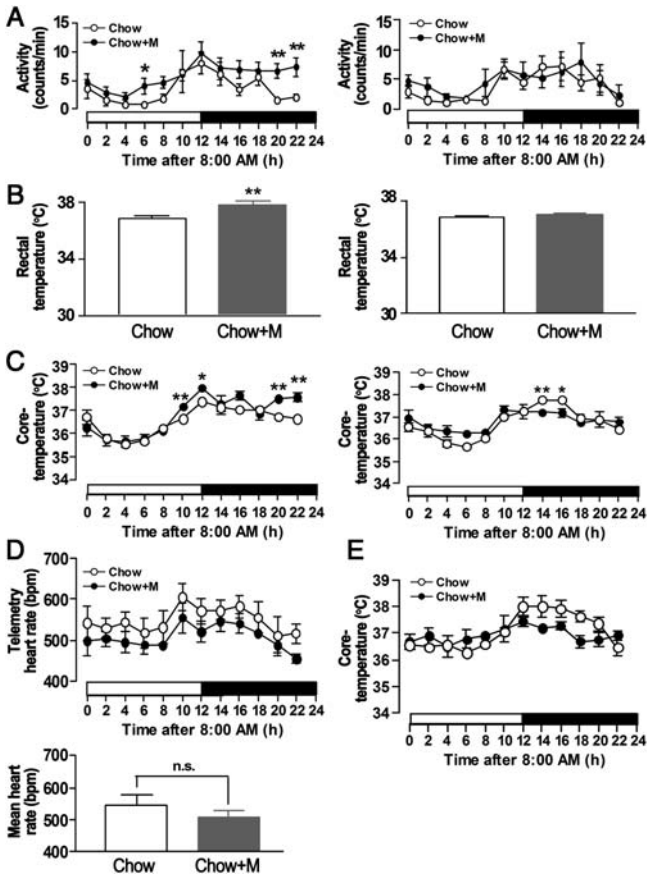

Figure 3 Menthol-enhanced UCP1-dependent thermogenesis and locomotor activity in mice. (**A**–**C**) Locomotor activity (**A**), rectal temperatures (**B**), and core body temperatures (**C**) of WT and TRPM8$^{-/-}$ mice fed on chow diet without (Chow) or with 0.5% menthol (Chow + M) for 7 months. *$P < 0.05$, **$P < 0.01$ vs. Chow. Data are expressed as mean ± SEM from six to eight mice per group. (**D**) The 24-h telemetry heart rates (top panel) and mean heart rates (bottom panel) of WT mice fed on chow diet without or with menthol. n.s. indicates $P > 0.05$. $n = 4$ per group. (**E**) The 24-h core body temperatures of UCP1$^{-/-}$ mice fed chow diet without (Chow) or with 0.5% menthol (Chow + M) for 7 months. $n = 6$ per group.

levels in mice treated with or without menthol for 7 months. Dietary menthol significantly increased oxygen consumption in WT mice but not in TRPM8$^{-/-}$ mice (Supplementary Figure S2), suggesting that dietary menthol increases the resting metabolic rate through TRPM8 activation. Although it is well known that the activation of β3-adrenergic receptor stimulates brown adipocyte proliferation and thermogenesis, mice lacking β3 receptors have been reported to maintain temperatures slightly below thermoneutrality. Furthermore, the levels of UCP1 in BAT were unchanged in these mice (Feldmann et al., 2009). This observation challenged the idea that the β-adrenoceptor signalling pathway is required for UCP1 expression (Uldry et al., 2006). Heart rate is a marker for β-adrenergic activity. However, heart rates were unchanged in mice treated with menthol (Figure 3D), which was consistent with *in vitro* results. Thyroid hormones are required for heat production stimulated by the sympathetic nervous system (Rubio et al., 1995; Ribeiro et al., 2001) and are among the regulators of UCP1 gene transcription (Martinez de Mena et al., 2010). However, our measurements revealed no differences in plasma levels of thyroid hormones in WT mice with and without menthol treatment (Supplementary Figure S3). This finding could constitute further evidence that long-term dietary menthol treatment affects UCP1-induced thermoregulation beyond the activation of the sympathetic nervous system. To demonstrate that TRPM8-mediated thermogenesis is dependent on UCP1, we determined that the core temperatures were not different between UCP1$^{-/-}$ mice with and without dietary menthol treatment (Figure 3E). The data indicated that the activation of TRPM8 significantly increased UCP1-dependent thermogenesis and locomotor activity, which is due to mechanisms that are beyond the activity of the sympathetic nervous system.

Dietary menthol prevents high-fat diet-induced obesity and glucose intolerance through TRPM8 activation

Active BAT is pivotal to maintain body temperature and to counteract diet-induced weight gain and the development of type 2 diabetes mellitus (Feldmann et al., 2009). Several studies have confirmed the presence of functional BAT in adult humans (Cypess et al., 2009; Saito et al., 2009; Virtanen et al., 2009). To assess whether TRPM8 activation can prevent obesity through UCP1-induced thermogenesis, we examined the effect of dietary menthol on high-fat diet (HFD)-induced obesity in mice. First, chronic dietary menthol prevented weight gain in WT mice on HFD, but this effect was absent in TRPM8$^{-/-}$ mice (Figure 4A). With the exception of the first day, the food intake amounts and faeces weights in WT mice with or without dietary menthol supplementation were all comparable (Supplementary Figure S4). This result showed that long-term dietary menthol treatment had no effect on food intake and faeces excretion. Secondly, core body temperatures were higher in WT mice on HFD plus menthol compared with WT mice on HFD alone over 24 h. There were significant differences during the period from 6:00 AM to 2:00 PM and at 8:00 PM (Figure 4B). Thirdly, menthol supplementation also significantly increased oxygen consumption levels in WT mice on HFD (Supplementary Figure S2). Fourthly, increased expression of UCP1 in BAT was identified in WT mice on HFD plus menthol compared with WT mice on HFD alone (Figure 4C). Furthermore, chronic dietary menthol treatment also attenuated HFD-induced glucose intolerance (Figure 4D) and improved insulin sensitivity (Figure 4E), as shown by intraperitoneal glucose tolerance and insulin tolerance tests. In contrast, the aforementioned effects were almost absent in TRPM8$^{-/-}$ mice on HFD (Figure 4B–E). These findings suggest that chronic dietary menthol treatment increases UCP1-dependent thermogenesis through TRPM8 activation, which combats dietary obesity and improves abnormal glucose homeostasis.

However, menthol had no significant effects on the 24-h locomotor activity in WT mice on HFD, with the only exception of the 4:00 PM time point (Supplementary Figure S5). The discrepancies in the activity rhythms and body temperatures in mice on HFD suggest that the thermoregulatory effects of menthol are not completely dependent on exercise-associated thermogenesis.

Diet-induced thermogenesis is another important factor that contributes to ~10% of total heat production. It has been

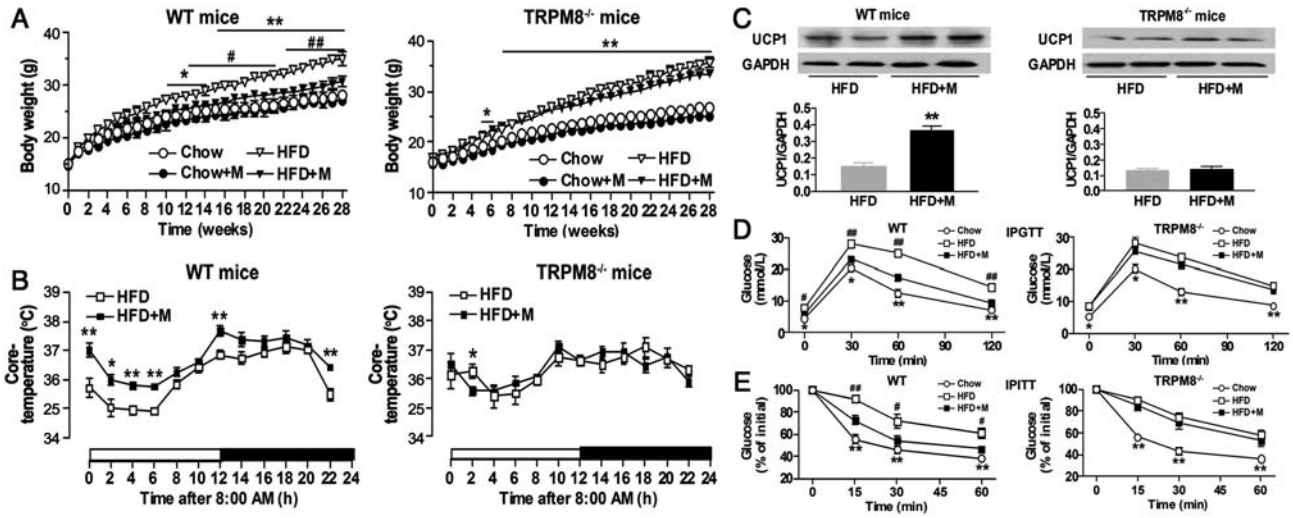

Figure 4 TRPM8 activation prevents HFD-induced obesity and glucose intolerance through UCP1-dependent thermogenesis. (**A**) The body weight gains of WT and TRPM8$^{-/-}$ mice fed chow diet (Chow) and HFD without or with menthol (HFD + M). *$P < 0.05$, **$P < 0.01$ vs Chow; $^{\#}P < 0.05$, $^{\#\#}P < 0.01$ vs HFD + M. $n = 6$ per group. (**B**) The 24-h core body temperatures of WT and TRPM8$^{-/-}$ mice fed HFD without or with menthol treatment. *$P < 0.05$, **$P < 0.01$ vs HFD. $n = 6$ per group. (**C**) UCP1 protein expression in the brown fat of WT and TRPM8$^{-/-}$ mice fed HFD with or without menthol. **$P < 0.01$ vs HFD. $n = 4$ per group. IPGTT (**D**) and IPITT (**E**) in WT and TRPM8$^{-/-}$ mice fed chow diet and HFD with or without menthol. *$P < 0.05$, **$P < 0.01$ vs HFD; $^{\#}P < 0.05$, $^{\#\#}P < 0.01$ vs HFD + M. $n = 4$ per group.

reported that diet-induced thermogenesis was inhibited in obese or insulin-resistant humans (Segal et al., 1992). However, we observed no differences in plasma insulin levels in mice on HFD with and without menthol treatment (Supplementary Figure S6).

Discussion

As a cold sensor, TRPM8 is activated by cold temperatures and pharmacological agents that mimic the psychophysical sensation of cold, such as menthol (Bautista et al., 2007; Cho et al., 2010). In general, cold stimuli enhance BAT activity through β-adrenergic signalling-mediated UCP1-induced thermogenesis (Feldmann et al., 2009). However, mice lacking β receptors have normal BAT with slight reductions in UCP1 levels and cold tolerance (Lehr et al., 2006), which suggests that an alternative pathway beyond adaptive adrenergic thermogenesis could be involved. In contrast to the classic view, we report here that TRPM8 functionally locates in BAT and can be activated by mimicking cold exposure using menthol, therefore enhancing UCP1-induced thermogenesis and locomotor activity. Furthermore, TRPM8 activation can protect against high-fat-induced obesity in mice but does not affect adrenergic activity. This finding suggests a novel pathway for UCP1-induced thermogenesis in BAT.

Recent studies have shown that adult humans possess active BAT, which is a source of potential interest for uncovering mechanisms to combat obesity through the manipulation of BAT (Fruhbeck et al., 2009a). Recently, the cascades of adipogenic transcription factors driving specific phenotypic features in adipocytes have received a great deal of attention (Yeh et al., 1995). C/EBP and PPARγ are the master regulators of adipogenesis (Lefterova et al., 2008). White and brown adipocytes are thought to be derived from the same precursor cell (Fruhbeck et al., 2009b). PR-domain-containing 16 (PRDM16) (Seale et al., 2008) and BMP7 (Tseng et al., 2008) have been recently identified as molecular switches that determine the formation and function of brown adipocytes. However, this study shows that PPARγ and BMP7 expression levels in BAT are not affected by menthol treatment in mice. Notably, brown adipocytes can emerge in WAT in response to chronic cold exposure or prolonged β-adrenergic stimulation (Fruhbeck et al., 2009a). However, the results of this study show that menthol treatment does not cause UCP1 expression, a unique biomarker for BAT, in WAT. These findings indicate that TRPM8 activation by menthol affects neither adipogenesis nor the formation of BAT.

Adaptive adrenergic thermogenesis represents BAT activity. UCP1, as the sole mediator of cold-induced non-shivering thermogenesis, is essential for mammals to maintain their body temperatures (Golozoubova et al., 2006). UCP1 is also a key contributor in the regulation of diet-induced thermogenesis (Feldmann et al., 2009). Our findings show that chronic dietary menthol increases UCP1 expression in BAT in WT mice but not in TRPM8$^{-/-}$ mice. Some studies have hinted that UCP1 activity and expression in BAT can be activated by p38/MAPK, AMPK, PI3K, and cAMP-dependent PKA (Robidoux et al., 2005; Tseng et al., 2008). In addition, PGC-1 is induced by cold exposure or adrenergic stimulation in BAT but not in WAT, and ectopic expression of PGC-1α in WAT induces the expression of UCP1 (Tseng et al., 2008). Our findings show that menthol treatment significantly increases the levels of p-PKA but not of PI3K, AMPK, or PGC-1 in brown adipocytes. Vogler et al. (2008) report that PKA phosphorylates the transcription factor CREB, which then supposedly activates the expression of UCP1. Interestingly, TRPM8 in HEK-293 cells can be regulated by the Gi protein/adenylate cyclase/cAMP/PKA signalling cascade (De Petrocellis et al., 2007; Bavencoffe et al., 2010). These findings suggest that TRPM8 activation can enhance BAT activity through PKA phosphorylation-mediated UCP1 expression.

Several recent studies suggest that increasing adaptive thermogenesis in BAT is a realistic tool for counteracting weight

gain (Tseng et al., 2008; Wijers et al., 2010; Yoneshiro et al., 2011). BAT is involved in cold-induced increases in whole-body energy expenditure and, therefore, in the control of body temperature and adiposity in adult humans (Yoneshiro et al., 2011). The absence of BAT may contribute to middle-age obesity. Obese subjects possess reduced cold-induced thermogenesis and energy expenditure compared with lean subjects (Claessens-van Ooijen et al., 2006). They showed that BAT activity was significantly lower in overweight or obese subjects during cold exposure. Both BMI and percentage of body fat had significant negative correlations with BAT whereas resting metabolic rate had a significant positive correlation (van Marken Lichtenbelt et al., 2009). Our findings show that chronic dietary menthol increases thermogenesis through the activation of TRPM8-mediated UCP1 production. In contrast, menthol treatment did not increase core temperatures in UCP1$^{-/-}$ mice. Furthermore, TRPM8 activation by menthol also markedly prevents dietary obesity and abnormal glucose homeostasis. Menthol treatment antagonizes the HFD-induced reduction of thermogenesis and energy expenditure and the down-regulation of UCP1 in BAT. Interestingly, the body weight was not different between mice on chow diet with and without menthol, although mice on dietary menthol have elevated activity and body temperature. This further confirmed that menthol mainly affected body fat, but not other compositions of body weight.

Tajino et al. (2011) recently reported that topical menthol application or cold temperature led to an increase in core body temperature that was dependent on TRPM8 expression and that TRPM8 expression was correlated with cold-induced UCP expression in BAT. However, for the first time, our study has demonstrated TRPM8 expression in brown adipocytes and has revealed a molecular pathway for TRPM8-dependent UCP1 expression. Although specific β3-adrenergic agonists can induce BAT activity and can activate thermogenesis in rodents, no metabolic effects of this agent were observed in a double-blinded, placebo-controlled randomized clinical study (Redman et al., 2007). Acute activation of TRPM8 induces both BAT and non-BAT-mediated heat-gain responses (Tajino et al., 2007). The present study cannot completely exclude some non-BAT-mediated effects in mice on long-term menthol diet.

Our study establishes a previously unrecognized role of cold-sensing TRPM8 in BAT function. TRPM8 agonists mimic a cold environment and could constitute a promising therapeutic approach for combating obesity and related metabolic disorders.

Materials and methods

Animals

We purchased WT (C57BL/6J) mice from Jackson Laboratory (Bar Harbor, ME, USA). We obtained TRPM8$^{-/-}$ mice from the lab of Dr Patapoutian (Dhaka et al., 2007) and obtained UCP1$^{-/-}$ mice from the Jackson Laboratory (Enerback et al., 1997). To maintain an isogenic strain, heterozygous knockout mice were propagated through breeding with WT C57BL/6J mice. We then intercross the heterozygous knockout mice to generate homozygous knockout mice and WT littermates which were identified by tail DNA PCR screening. These homozygous knockout mice and their WT littermates were maintained and used for experiments. Animals, 6–8 weeks of age, were housed under controlled temperature (21°C–23°C), with a 12/12 h light-dark cycle (lights on 06:00 to 18:00), and were randomly divided into four groups and received standard chow diet (Chow), chow diet plus 0.5% menthol (Chow + M), HFD and HFD plus 0.5% menthol (HFD + M) for 28 weeks. Body weights were measured every week. At the end of 28 weeks, the mice were sacrificed and BATs were used for measurement. All of the experimental procedures were performed in accordance with protocols approved by the Institutional Animal Care and Research Advisory Committee.

Primary cell culture

Adipose tissue was processed, including the careful removal of fibrous tissue and blood vessels, followed by collagenase digestion. After centrifugation, floating mature adipocytes were separated from the stromal-vascular cell pellet, which was subjected to additional filtrations (25 mm final pore size) to yield the preadipocytes fraction. Cells were cultured and maintained in Dulbecco's modified Eagle's medium supplemented with 10% fetal calf serum (HyClone) containing 100 μg/ml penicillin and 100 μg/ml streptomycin (Gibco). Cells were treated with menthol at varying concentrations (30, 100, 300 μM) and vehicle as control for 24 h.

Fluorescence measurement of cytosolic free calcium

Cytosolic free calcium concentration ($[Ca^{2+}]_i$) was measured by using a fluorescence dye Fura-2 AM according to previously published techniques by our group (Zhang et al., 2007). Cells grown on glass cover slips were loaded with 2 μM of Fura-2 AM (Sigma-Aldrich) and 0.025% Pluronic F-127 in physiological saline solution (PSS) containing 135 mM NaCl, 5 mM KCl, 1.5 mM $CaCl_2$, 1 mM $MgCl_2$, 11 mM D-glucose and 10 mM HEPES, pH 7.4, for 45 min at 37°C in the dark. Cells were then washed with PSS three times to remove extraneous dye. Fluorescence at baseline and after menthol stimulation was measured at 510 nm emission with excitation wavelengths of 340 nm and 380 nm using the PTI Fluorescence Master Systems (Photon Technology International). The $[Ca^{2+}]_i$ was expressed as the ratio of F340 nm/F380 nm. The increase of the ratio was calculated from the maximum value after stimulation minus the average baseline value.

Western blot analysis

Immunoblots of TRPM8, UCP1, PKA, p-PKA, PPARγ, PGC-1, BMP7, and GAPDH were as described [(Yan et al., 2007; Liu et al., 2009; He et al., 2010). Tissues were homogenized and cells were lysed in high-salt extraction buffer (0.5 M Tris, 1% NP-40, 1% Triton X-100, 1 g/L sodium dodecyl sulfate, 1.5 M NaCl, 0.2 M ethylenediaminetetraacetic acid, and 0.01 M ethylene glycol bis(2-aminoethyl) tetraacetic acid (EGTA)] and placed at −20°C for 20 min. The protein supernatants were separated by centrifugation at 12000 *g* for 20 min at 4°C, and protein concentrations were determined with Bio-Rad protein assay reagent (Bio-Rad). Equal amounts of proteins were separated by using 10% SDS–PAGE and transferred to polyvinylidene difluoride membranes at 90 mA. After Transfer, membranes were blocked for 4 h at room temperature in blocking buffer (Bio-Rad). Next, the membranes were incubated overnight at 4°C with primary antibodies for TRPM8 (Alomone) and others (Santa Cruz Biotechnology). After incubation with secondary antibodies

(ZSGB-BIO) at room temperature for 2 h, the proteins were detected with enhanced chemiluminescence and quantified using a Gel Doc 2000 Imager (Bio-Rad). Protein expression was normalized to the internal control GAPDH.

Immunofluorescence staining

The immunofluorescence staining of brown adipocytes was as previously described (Yang et al., 2010). Cells were fixed with 10% formalin for 30 min at room temperature, incubated with PBS containing 5% bovine serum for 30 min at room temperature. Then cells were incubated with TRPM8 antibody (NOVUS Biologicals) and UCP1 antibody (Santa Cruz Biotechnology) overnight at 4°C, washed with PBS and incubated with antibodies conjugated to a fluorescent probe (ZSGB-BIO) for 30 min at room temperature in the dark. Control experiments were performed in the absence of primary antibodies. After removing the unbound secondary antibodies by washing the preparations with PBS, imaging was performed using the fluorescence microscope (TE2000; Nikon).

Measurement of temperature and locomotor activity

Rectal temperature of mice was measured by the rectal probe digital thermometer (Physitemp) inserted 1.8 cm into the colon and the measurement was performed during 9:00 AM to 10:00 AM every time. The core body temperature and the locomotor activity were simultaneously measured by the telemetry system (TA10TA-F20; Data Sciences, Inc.). Surgical preparation for implanting telemetry device was as described (Moore and Fewell, 2006). Mice were anaesthetized by inducing 2% halothane in oxygen, and then maintained via mask using an open-circuit anaesthesia system delivering 2% halothane in oxygen at 1 L/min. A paramedian laparotomy was performed utilising aseptic technique and telemetry was placed in the peritoneal cavity for measurement of core temperature and locomotor activity. During recovery from anaesthesia, mice were placed on a heating pad (32°C). After the mice had recovered from anaesthesia, they were returned to cages for a 1-week recovery period before the initiation of recording.

Telemetry heart rate measurement

Heart rate was measured by the telemetry system (TA11PA-C10; Data Sciences, Inc.). Surgical protocols were described as following. Mice were anaesthetized as described above. A vertical incision was made in the left axillary space. The main body of the telemetry probe was inserted subcutaneously and secured by suturing to the skin. A vertical incision was then made on the neck (right front side) and the tips of fine haemostats were advanced underneath the skin to the incision in axillary space. The flexible tip of the probe catheter was gently grasped, pulled, and protruded through the incision on the neck. The right common carotid artery was then isolated with blunt dissection and ligated with suture (5–0 silk) at the site of bifurcation into the internal and external branches. This suture was then retracted toward the head. An additional suture was placed around the common carotid artery 8–10 mm below the bifurcation, and blood flow was occluded by retracting this suture toward the tail. The tip of the probe catheter was inserted into the carotid lumen using a needle as an introducer, and the needle was then withdrawn and the tip of the catheter advanced to the point of the occlusion suture. The catheter was secured with Vetbond and the occluding suture was released. A small piece of cellulose patch was placed over the catheter and fixed with Vetbond to secure the catheter. The incision was closed with suture and surgical staples. During recovery from anaesthesia, mice were placed on a heating pad (32°C). After the mice had recovered from anaesthesia, they were returned to cages for a 1-week recovery period before the initiation of recording. The mean heart rate was calculated according to the 24-h data for each mouse.

Intraperitoneal glucose tolerance and insulin tolerance tests

Intraperitoneal glucose tolerance test (IPGTT) was carried out as previously described (Sun et al., 2007). After an overnight fast (14 h), glucose (2 g/kg body weight) was administered via injection into the peritoneal cavity, and blood was obtained from the tail at 0, 30, 60 and 120 min after glucose administration. Blood glucose levels were determined using the OneTouch Ultra blood glucose meter (LifeScan). Intraperitoneal insulin tolerance test (IPITT) was evaluated in fed mice on a different day. Humulin R (0.75 U/kg body wt) (Eli Lilly and Co.) in sterile saline was administered via injection into the peritoneal cavity. Glucose levels were determined in the tail blood at 0, 15, 30 and 60 min after insulin injection.

Statistical analyses

All data from mice are expressed as mean ± SEM. Comparisons between groups were analysed by using one-way analysis of variance with Bonferroni's multiple comparison *post hoc* tests or Student's *t*-test, as appropriate. We considered $P < 0.05$ statistically significant.

Supplementary material

Supplementary material is available at *Journal of Molecular Cell Biology* online.

Acknowledgements

We thank Dr Yu Huang (Chinese University of Hong Kong, China) and Dr Freichel (University of Saarland, Germany) for constructive comments of the manuscript. We acknowledge Dr Patapoutian (The Scripps Research Institute, CA, USA) and Dr Chengyu Zhang (Nanjing University, China) for providing the gene knockout mice. We thank Lijuan Wang and Tingbing Cao for skillful technical assistance.

Funding

This work was supported by grants from the National Basic Research Program of China (2012CB517805 and 2012CB517806), the National Natural Science Foundation of China (30890042). This work was also supported by the Program for Changjiang Scholars from the Ministry of Education in China.

Conflicts of interest: none declared.

References

Bautista, D.M., Siemens, J., Glazer, J.M., et al. (2007). The menthol receptor TRPM8 is the principal detector of environmental cold. Nature *448*, 204–208.

Bavencoffe, A., Gkika, D., Kondratskyi, A., et al. (2010). The transient receptor potential channel TRPM8 is inhibited via the alpha 2A adrenoreceptor signaling pathway. J. Biol. Chem. *285*, 9410–9419.

Cannon, B., and Nedergaard, J. (2004). Brown adipose tissue: function and physiological significance. Physiol. Rev. *84*, 277–359.

Cho, Y., Jang, Y., Yang, Y.D., et al. (2010). TRPM8 mediates cold and menthol allergies associated with mast cell activation. Cell Calcium *48*, 202–208.

Christian, M., and Parker, M.G. (2010). The engineering of brown fat. J. Mol. Cell Biol. *2*, 23–25.

Claessens-van Ooijen, A.M., Westerterp, K.R., Wouters, L., et al. (2006). Heat production and body temperature during cooling and rewarming in overweight and lean men. Obesity (Silver Spring) *14*, 1914–1920.

Colburn, R.W., Lubin, M.L., Stone, D.J. Jr., et al. (2007). Attenuated cold sensitivity in TRPM8 null mice. Neuron *54*, 379–386.

Cypess, A.M., Lehman, S., Williams, G., et al. (2009). Identification and importance of brown adipose tissue in adult humans. N. Engl. J. Med. *360*, 1509–1517.

De Petrocellis, L., Starowicz, K., Moriello, A.S., et al. (2007). Regulation of transient receptor potential channels of melastatin type 8 (TRPM8): effect of cAMP, cannabinoid CB(1) receptors and endovanilloids. Exp. Cell Res. *313*, 1911–1920.

Dhaka, A., Murray, A.N., Mathur, J., et al. (2007). TRPM8 is required for cold sensation in mice. Neuron *54*, 371–378.

Enerback, S. (2010). Human brown adipose tissue. Cell Metab. *11*, 248–252.

Enerback, S., Jacobsson, A., Simpson, E.M., et al. (1997). Mice lacking mitochondrial uncoupling protein are cold-sensitive but not obese. Nature *387*, 90–94.

Feldmann, H.M., Golozoubova, V., Cannon, B., et al. (2009). UCP1 ablation induces obesity and abolishes diet-induced thermogenesis in mice exempt from thermal stress by living at thermoneutrality. Cell Metab. *9*, 203–209.

Fredriksson, J.M., Thonberg, H., Ohlson, K.B., et al. (2001). Analysis of inhibition by H89 of UCP1 gene expression and thermogenesis indicates protein kinase A mediation of beta(3)-adrenergic signalling rather than beta(3)-adrenoceptor antagonism by H89. Biochim. Biophys. Acta *1538*, 206–217.

Frontini, A., and Cinti, S. (2010). Distribution and development of brown adipocytes in the murine and human adipose organ. Cell Metab. *11*, 253–256.

Fruhbeck, G., Becerril, S., Sainz, N., et al. (2009a). BAT: a new target for human obesity? Trends Pharmacol. Sci. *30*, 387–396.

Fruhbeck, G., Sesma, P., and Burrell, M.A. (2009b). PRDM16: the interconvertible adipo-myocyte switch. Trends Cell Biol. *19*, 141–146.

Golozoubova, V., Cannon, B., and Nedergaard, J. (2006). UCP1 is essential for adaptive adrenergic nonshivering thermogenesis. Am. J. Physiol. Endocrinol. Metab. *291*, E350–E357.

He, H., Yang, D., Ma, L., et al. (2010). Telmisartan prevents weight gain and obesity through activation of peroxisome proliferator-activated receptor-delta-dependent pathways. Hypertension *55*, 869–879.

Karamitri, A., Shore, A.M., Docherty, K., et al. (2009). Combinatorial transcription factor regulation of the cyclic AMP-response element on the Pgc-1alpha promoter in white 3T3-L1 and brown HIB-1B preadipocytes. J. Biol. Chem. *284*, 20738–20752.

Lefterova, M.I., Zhang, Y., Steger, D.J., et al. (2008). PPARgamma and C/EBP factors orchestrate adipocyte biology via adjacent binding on a genome-wide scale. Genes Dev. *22*, 2941–2952.

Lehr, L., Canola, K., Asensio, C., et al. (2006). The control of UCP1 is dissociated from that of PGC-1alpha or of mitochondriogenesis as revealed by a study using beta-less mouse brown adipocytes in culture. FEBS Lett. *580*, 4661–4666.

Li, Y., Zhang, J., Schopfer, F.J., et al. (2008). Molecular recognition of nitrated fatty acids by PPAR gamma. Nat. Struct. Mol. Biol. *15*, 865–867.

Lidell, M.E., and Enerback, S. (2010). Brown adipose tissue—a new role in humans? Nat. Rev. Endocrinol. *6*, 319–325.

Liu, D., Yang, D., He, H., et al. (2009). Increased transient receptor potential canonical type 3 channels in vasculature from hypertensive rats. Hypertension *53*, 70–76.

Mahieu, F., Owsianik, G., Verbert, L., et al. (2007). TRPM8-independent menthol-induced Ca^{2+} release from endoplasmic reticulum and Golgi. J. Biol. Chem. *282*, 3325–3336.

Martinez de Mena, R., Scanlan, T.S., and Obregon, M.J. (2010). The T3 receptor beta1 isoform regulates UCP1 and D2 deiodinase in rat brown adipocytes. Endocrinology *151*, 5074–5083.

McKemy, D.D., Neuhausser, W.M., and Julius, D. (2002). Identification of a cold receptor reveals a general role for TRP channels in thermosensation. Nature *416*, 52–58.

Moore, S.L., and Fewell, J.E. (2006). Mifepristone (RU38486) influences the core temperature response of term pregnant rats to intraperitoneal lipopolysaccharide. Exp. Physiol. *91*, 741–746.

Nedergaard, J., and Cannon, B. (2010). The changed metabolic world with human brown adipose tissue: therapeutic visions. Cell Metab. *11*, 268–272.

Nedergaard, J., Ricquier, D., and Kozak, L.P. (2005). Uncoupling proteins: current status and therapeutic prospects. EMBO Rep. *6*, 917–921.

Nedergaard, J., Bengtsson, T., and Cannon, B. (2011). New powers of brown fat: fighting the metabolic syndrome. Cell Metab. *13*, 238–240.

Nilius, B., and Voets, T. (2007a). Neurophysiology: channelling cold reception. Nature *448*, 147–148.

Nilius, B., Owsianik, G., Voets, T., et al. (2007b). Transient receptor potential cation channels in disease. Physiol. Rev. *87*, 165–217.

Peier, A.M., Moqrich, A., Hergarden, A.C., et al. (2002). A TRP channel that senses cold stimuli and menthol. Cell *108*, 705–715.

Redman, L.M., de Jonge, L., Fang, X., et al. (2007). Lack of an effect of a novel beta3-adrenoceptor agonist, TAK-677, on energy metabolism in obese individuals: a double-blind, placebo-controlled randomized study. J. Clin. Endocrinol. Metab. *92*, 527–531.

Ribeiro, M.O., Carvalho, S.D., Schultz, J.J., et al. (2001). Thyroid hormone-sympathetic interaction and adaptive thermogenesis are thyroid hormone receptor isoform-specific. J. Clin. Invest. *108*, 97–105.

Robidoux, J., Cao, W., Quan, H., et al. (2005). Selective activation of mitogen-activated protein (MAP) kinase kinase 3 and p38alpha MAP kinase is essential for cyclic AMP-dependent UCP1 expression in adipocytes. Mol. Cell. Biol. *25*, 5466–5479.

Rousset, S., Alves-Guerra, M.C., Mozo, J., et al. (2004). The biology of mitochondrial uncoupling proteins. Diabetes *53(Suppl 1)*, S130–S135.

Rubio, A., Raasmaja, A., Maia, A.L., et al. (1995). Effects of thyroid hormone on norepinephrine signaling in brown adipose tissue. I. Beta 1- and beta 2-adrenergic receptors and cyclic adenosine 3′,5′-monophosphate generation. Endocrinology *136*, 3267–3276.

Saito, M., Okamatsu-Ogura, Y., Matsushita, M., et al. (2009). High incidence of metabolically active brown adipose tissue in healthy adult humans: effects of cold exposure and adiposity. Diabetes *58*, 1526–1531.

Seale, P., Bjork, B., Yang, W., et al. (2008). PRDM16 controls a brown fat/skeletal muscle switch. Nature *454*, 961–967.

Seale, P., Kajimura, S., and Spiegelman, B.M. (2009). Transcriptional control of brown adipocyte development and physiological function—of mice and men. Genes Dev. *23*, 788–797.

Segal, K.R., Albu, J., Chun, A., et al. (1992). Independent effects of obesity and insulin resistance on postprandial thermogenesis in men. J. Clin. Invest. *89*, 824–833.

Speakman, J.R. (2010). FTO effect on energy demand versus food intake. Nature *464*, E1; discussion E2.

Sun, C., Zhang, F., Ge, X., et al. (2007). SIRT1 improves insulin sensitivity under insulin-resistant conditions by repressing PTP1B. Cell Metab. *6*, 307–319.

Sweeting, H.N. (2008). Gendered dimensions of obesity in childhood and adolescence. Nutr. J. *7*, 1.

Tajino, K., Matsumura, K., Kosada, K., et al. (2007). Application of menthol to the skin of whole trunk in mice induces autonomic and behavioral heat-gain responses. Am. J. Physiol. Regul. Integr. Comp. Physiol. *293*, R2128–R2135.

Tajino, K., Hosokawa, H., Maegawa, S., et al. (2011). Cooling-sensitive TRPM8 is thermostat of skin temperature against cooling. PLoS One *6*, e17504.

Tseng, Y.H., Kokkotou, E., Schulz, T.J., et al. (2008). New role of bone morphogenetic protein 7 in brown adipogenesis and energy expenditure. Nature *454*, 1000–1004.

Uldry, M., Yang, W., St-Pierre, J., et al. (2006). Complementary action of the PGC-1 coactivators in mitochondrial biogenesis and brown fat differentiation. Cell Metab. *3*, 333–341.

van Marken Lichtenbelt, W.D., Vanhommerig, J.W., Smulders, N.M., et al. (2009). Cold-activated brown adipose tissue in healthy men. N. Engl. J. Med. *360*, 1500–1508.

Virtanen, K.A., Lidell, M.E., Orava, J., et al. (2009). Functional brown adipose tissue in healthy adults. N. Engl. J. Med. *360*, 1518–1525.

Voets, T., Droogmans, G., Wissenbach, U., et al. (2004). The principle of temperature-dependent gating in cold- and heat-sensitive TRP channels. Nature *430*, 748–754.

Voets, T., Owsianik, G., Janssens, A., et al. (2007). TRPM8 voltage sensor mutants reveal a mechanism for integrating thermal and chemical stimuli. Nat. Chem. Biol. *3*, 174–182.

Vogler, O., Lopez-Bellan, A., Alemany, R., et al. (2008). Structure-effect relation of C18 long-chain fatty acids in the reduction of body weight in rats. Int. J. Obes. (Lond.) *32*, 464–473.

Wijers, S.L., Saris, W.H., and van Marken Lichtenbelt, W.D. (2010). Cold-induced adaptive thermogenesis in lean and obese. Obesity (Silver Spring) *18*, 1092–1099.

Yan, Z.C., Liu, D.Y., Zhang, L.L., et al. (2007). Exercise reduces adipose tissue via cannabinoid receptor type 1 which is regulated by peroxisome proliferator-activated receptor-delta. Biochem. Biophys. Res. Commun. *354*, 427–433.

Yang, D., Luo, Z., Ma, S., et al. (2010). Activation of TRPV1 by dietary capsaicin improves endothelium-dependent vasorelaxation and prevents hypertension. Cell Metab. *12*, 130–141.

Yeh, W.C., Cao, Z., Classon, M., et al. (1995). Cascade regulation of terminal adipocyte differentiation by three members of the C/EBP family of leucine zipper proteins. Genes Dev. *9*, 168–181.

Yoneshiro, T., Aita, S., Matsushita, M., et al. (2011). Brown adipose tissue, whole-body energy expenditure, and thermogenesis in healthy adult men. Obesity (Silver Spring) *19*, 13–16.

Zhang, L.L., Yan Liu, D., Ma, L.Q., et al. (2007). Activation of transient receptor potential vanilloid type-1 channel prevents adipogenesis and obesity. Circ. Res. *100*, 1063–1070.